Structured ground states of randomly interacting bosons

Charles White [1], Alexander Volya [1], Declan Mulhall [2], and Vladimir Zelevinsky [3]
[1]*Department of Physics, Florida State University, Tallahassee, Florida 32306, USA*
[2]*Department of Physics and Engineering, University of Scranton, Scranton, Pennsylvania 18510-4642, USA*
[3]*Department of Physics and Astronomy and Facility for Rare Isotope Beams, Michigan State University, East Lansing, Michigan 48824-1321, USA*

(Received 15 November 2022; accepted 3 February 2023; published 13 February 2023)

Bosonic degrees of freedom and their emergence as part of complex quantum many-body dynamics, symmetries, collective behavior, clustering, and phase transitions play an important role in modern studies of quantum systems. In this paper, we present a systematic study of many-boson systems governed by random interactions. Our findings show that ground states of randomly interacting bosons are not random, being dominated by a few collective configurations containing condensates of clusters.

DOI: 10.1103/PhysRevResearch.5.013109

I. INTRODUCTION

Quantum many-body systems display a variety of remarkable phenomena that emerge as a result of simple interactions among the constituents. Bosonic degrees of freedom and their interactions play an important part in the emergent phenomena. In this paper, we address the generic features exhibited by randomly interacting systems of bosons. The revolutionary ideas about statistical properties of quantum systems date back to the Gaussian orthogonal ensemble of random matrices introduced by Wigner [1–3], who proposed that a random matrix ensemble invariant with respect to the choice of basis be used to describe complex, or chaotic in modern terminology, quantum systems. Random matrix theory is a powerful and widely used modern-day tool; for overview, see Refs. [4–6] and references therein. The well-known physics of many realistic systems, especially at relatively low excitation energies, suggest that low-rank embedded ensembles [7] and, in particular, two-body random ensembles are quite relevant [8–12]. For numerous realistic atomic and nuclear systems [5,13,14], high level density leads to strong mixing of basis states, and the observable properties approach those given by the predictions of random matrix ensembles.

Over the last two decades, the question of the emergence of regularities out of chaos has been a particularly interesting and rapidly developing topic. One of the main highlights is an observation of an unusually high likelihood for the ground state of a random system to have zero spin [15]. This remains true even if the two-body interaction does not favor pairing or any other obvious force favorable to a net-zero angular momentum arrangement. Multiple further investigations have followed [5,15–24] and many more remarkable features that emerge out of chaos have been found. In fermionic systems, the emergence of rotational and vibrational regularities [17,24] naturally connects this topic to the interacting boson model [25] and to the more in-depth questions of higher symmetries [20,26,27] known to be intrinsic to bosonic systems and dynamics of shape and phase transitions [28].

While bosonic systems have been discussed for a while [20,29], there has been a resurgence of interest [30–32] because of the importance that bosons play in our general understanding of emergent phenomena, such as symmetries, formation of effective degrees of freedom, clustering, and collective dynamics that include pairing and phase transitions.

In this paper, we study bosonic systems with two-body random interactions. We limit the scope to systems of identical bosons, although our results are likely to be valid more generally. We also limit our consideration to ground states. Other properties, such as emergence of bands and transitions, will be discussed elsewhere.

II. BOSONIC RANDOM ENSEMBLE

We consider a system of N identical bosons with integer spin ℓ that interact via the most general two-body Hamiltonian:

$$H = \sum_{L=0,2,4\ldots}^{2\ell} V_L \sum_{M} P^{\dagger}_{LM} P_{LM}. \tag{1}$$

The $P^{\dagger}_{LM}$ and P_{LM} are boson pair creation and annihilation operators with angular momentum L and magnetic projection M. We normalize them so a pair state created from the vacuum by any of the operators $P^{\dagger}_{LM}$ is normalized to one. Since the bosons are identical, they can only be in a symmetric state, which requires L to be even.

How the many-boson states can be classified in terms of the rotational group and, specifically for a system of N bosons with spin ℓ, how many states there are with total spin J,

labeled as $D_{\ell N}(J)$, are important and nontrivial questions. For completeness of this presentation, we review this subject in Appendix A; additional information can be found in the textbook [33]. In certain cases, $D_{\ell N}(J)$ is known analytically; generally, as a function of J it is a peaked curve, so the number of states with low and high spins is small, see Fig. 14. Cases of unique states $D_{\ell N}(J) = 1$, which include the aligned state of maximum spin $J_{\max} = \ell N$, are special as in these cases the energy is a linear function of the interaction parameters V_L.

For the two-body random forces, we assume an ensemble of Hamiltonians where the matrix elements V_L of the two-body interaction are selected at random from a normal distribution so

$$\overline{V_L} = 0 \quad \text{and} \quad \overline{V_L^2} = 1. \tag{2}$$

There are also the well-known special two-body Hamiltonians: pairing, monopole, and square of the total angular momentum operator, which we review in more detail in Appendix B, see also Ref. [33]. The monopole operator, which is related to the number of particles, and the angular momentum operator squared both commute with any Hamiltonian; thus, we remove these collective components from each realization of Hamiltonian Eq. (1), resulting in the slightly modified Hamiltonian H' of the ensemble, which we refer to collectively as the primed ensemble. The exact procedure is discussed in Appendix C. Clearly, the wave functions do not change; the monopole term only shifts the overall energy while the J^2 term gives a contribution proportional to $J(J+1)$ to the energy of each state. We found no significant difference in the results that are of interest from the removal of the two collective components; however, doing this helps to address a potential concern related to these collective terms dominating the statistics, see Ref. [34].

For each random realization of the Hamiltonian, we study its ground-state wave function, energy, spin, and other properties for systems with different numbers of particles. We also explore correlations and multiboson transitions between the ground states of different-sized systems. Numerical results for various systems that we discuss throughout this paper are shown in Table II. Unless otherwise noted, the results in each case come from an ensemble of 100 000 realizations. The first three columns identify the boson spin ℓ, number of bosons N, and the spin of interest J, the fourth column shows the number of states with this spin in the system $D_{\ell N}(J)$, and the fifth column gives the total number of spin states $D = \sum_J D_{\ell N}(J)$. We discuss other columns as we continue with our presentation.

III. GROUND STATE SPIN PROBABILITY DISTRIBUTION

We begin with a discussion of the ground-state spin distribution in Figs. 1 and 2, which show the probability $P(J)$ of the ground state having spin J in eight- and seven-particle systems of $\ell = 5$ bosons, respectively. This is a known result, discussed previously by many authors, and is surprisingly similar to the systematics found in fermionic systems. Following are some of the key observations. In a large number of cases, typically between 30 to 50%, the ground-state spin is equal to either zero for an even number of bosons or to ℓ (the spin of an individual boson) if the number of bosons is odd. In disproportionately many cases, the ground state has the maximum angular momentum possible: $J_{\max} = N\ell$. The probability of $J = J_{\max} - N = (\ell - 1)N$ is also enhanced. The results for $P(J)$ from numerical studies using the primed ensemble are shown in the sixth column of Table II.

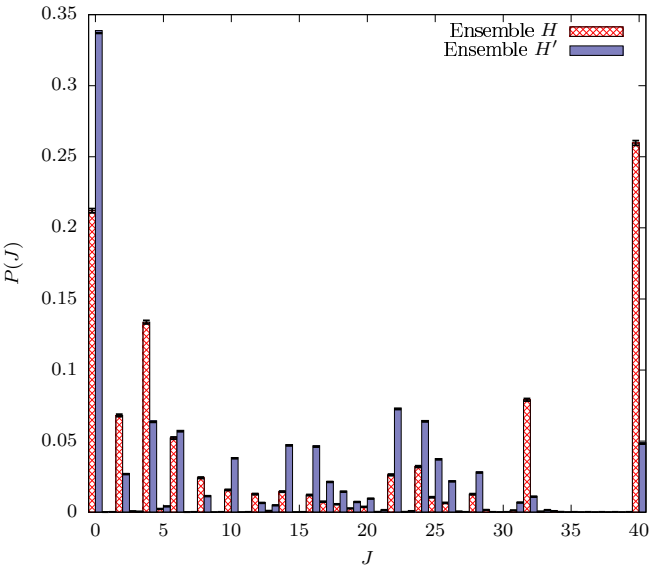

FIG. 1. Comparison of ground-state spin distribution for the original and primed ensembles of 100 000 Hamiltonians. System of $N = 8$ bosons with spin $\ell = 5$ is considered. The (very small) statistical error for each spin is shown by an error bar.

The likelihood of the ground state being aligned with a maximal spin is affected by the collective J^2 term; removal of this term reduces $P(J_{\max})$. The maximally aligned state represents a condensate of aligned bosons with energy fully

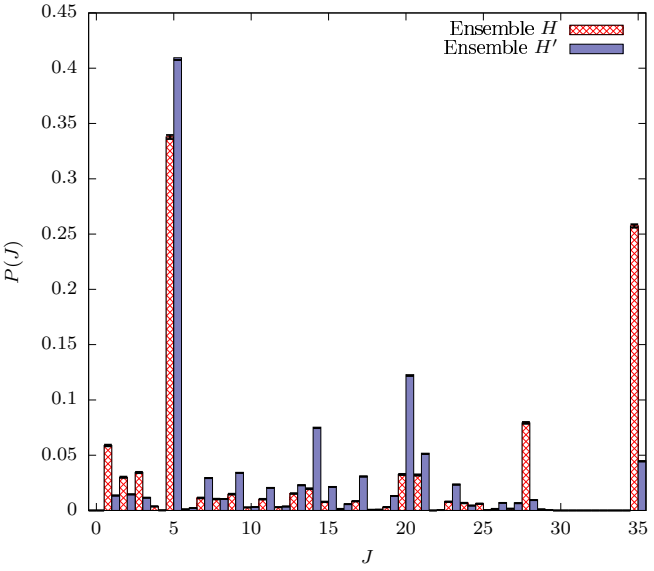

FIG. 2. Comparison of ground-state spin distribution for the original and primed ensembles of 100 000 Hamiltonians. System of $N = 7$ bosons with spin $\ell = 5$ is considered. The (very small) statistical error for each spin is shown by an error bar.

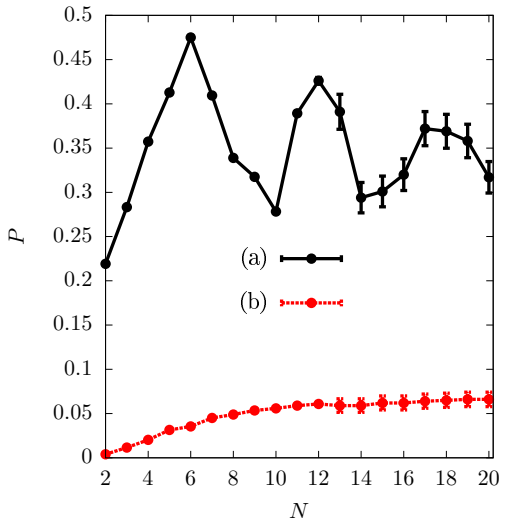

FIG. 3. For bosons with spin $\ell = 5$, the probability of observing a ground state of a certain spin J is shown as a function of boson number N. Line (a) shows the probability of the ground state spin $J = 0$ for even N and $J = \ell$ for odd N. Line (b) shows the probability of $J_{\max} = N\ell$. To expedite our studies for systems with $N > 12$, ensembles of 1000 Hamiltonians were used instead of 100 000, which resulted in noticeable statistical error shown with the error bars.

determined by a single matrix element $V_{2\ell}$:

$$E = \tfrac{1}{2}N(N-1)V_{2\ell}. \tag{3}$$

Being collectively scaled with the number of particles and dependent on this single matrix element, the enhancement $P(J_{\max})$ is not unexpected, although there is no answer for an exact probability. Some assessments based on extreme eigenvalue deviations can be made [35]. Other high-spin states with enhanced chances to appear in the ground state are also structurally very simple and generally depend only on the few matrix elements V_L with largest L. This is evident from the comparison of the original and primed ensembles in Figs. 1 and 2. The behavior of $P(0)$, $P(\ell)$, and $P(J_{\max})$ for a system of bosons with spin $\ell = 5$ as a function of the boson number N is shown in Fig. 3.

IV. EXAMPLE OF *d* BOSONS

As an introductory discussion, in this section we present the analytically solvable case of $\ell = 2$, d bosons. This problem is analytically solvable thanks to the additional symmetry that brings in a conserved quantum number. Details of bosonic algebras can be found in a number of references [33,36–38]. The spin statistics of ground states for a d-boson system can be determined analytically [20,30] because there are enough quantum numbers to make the eigenvalues of the Hamiltonian linear functions of the two-body interaction parameters V_L, Eq. (10). This is an instructive example that helps guide our discussion that follows.

For a given N, the number of unpaired particles (called seniority) can be $\nu = N,\ N-2,\ N-4, \ldots$, with the smallest value being 0 or 1 if the number of particles is, correspondingly, even or odd. Any Hamiltonian for d bosons commutes with the pairing Hamiltonian, making seniority ν a good quantum number. Then, among ν unpaired particles, we can have some triplets that are coupled to zero angular momentum; thus, the number f of free particles that are neither in pairs nor in triplets is $f = \nu,\ \nu-3,\ \nu-6, \ldots$, with the smallest number being the remainder from division of ν by 3 (modulo). These uncoupled f particles are the ones producing the angular momentum,

$$J = 2f,\ 2f-2,\ 2f-3,\ 2f-4, \ldots,\ f, \tag{4}$$

which can take all integer values between $2f$ and f with the exception of $2f-1$.

Thanks to seniority being conserved, all states can be uniquely identified by their spin and seniority. Thus, the energy from Hamiltonian Eq. (1) is a linear function of the three interaction parameters V_0, V_2, and V_4. The energy for N d-bosons as a function of seniority and angular momentum is

$$E(\nu, J) = -\beta\nu(\nu+3) + \gamma J(J+1), \tag{5}$$

where the coefficients β and γ are given in terms of the two-body matrix elements:

$$\beta = \tfrac{1}{10}V_0 - \tfrac{1}{7}V_2 + \tfrac{3}{70}V_4, \tag{6}$$

$$\gamma = \tfrac{1}{14}(V_4 - V_2). \tag{7}$$

Here we disregard some constant terms that depend only on the number of particles. With only three interaction parameters, any Hamiltonian can always be written as a linear combination of pairing, monopole, and angular momentum squared terms, which provides an alternative perspective on the result. See Appendix B.

Assuming that the parameters V_L obey a normal distribution, the joint probability distribution for β and γ is

$$P(\beta, \gamma) = \frac{70}{\sqrt{3}\pi} \exp\left(-\frac{4}{3}(25\beta^2 - 65\beta\gamma + 79\gamma^2)\right). \tag{8}$$

From this, we can find various probabilities; for example, the probability for the case where β and γ are both positive (same for both negative) is

$$P(\beta > 0, \gamma > 0) = \frac{1}{4} + \frac{1}{2\pi}\arctan\left(\frac{13}{7\sqrt{3}}\right) \approx 0.38. \tag{9}$$

These rules provide a direct strategy for determining $P(J)$. We will not go into the details of the analytical analysis built around Eq. (8), the results can be found in Ref. [30]. Because of pair and triplet clusters, the systematics have a periodicity of 6 in the number of particles. This periodicity becomes exact in the asymptotic limit of large N. The ground-state spin can only be $J = 0$, $J = 2$, or $J = 2N$; the asymptotic probabilities $P(J)$ over the period are summarized in Table I.

To summarize this analytic example, the ground states of d-boson systems are combined from spin-zero pairs and triplets or are condensates of aligned bosons in the case of $J_{\max}$. Because interactions are of the two-body type, the triplets of spin zero do not explicitly contribute to the energy and, depending on if pairing interaction is attractive or repulsive, the seniority is correspondingly minimized or maximized. This clustering

TABLE I. Table shows asymptotic probabilities ($N \gg 1$), which have a periodicity of 6 in the particle number, to see ground state of spin $J = 0$, $J = \ell = 2$, and $J = J_{\max} = 2N$ for d bosons. Probabilities are expressed in percentage. Integer k denotes the period.

N	$P(0)$	$P(2)$	$P(J_{\max})$
$6k$	57	0	43
$6k \pm 1$	2	55	43
$6k \pm 2$	19	38	43
$6k \pm 3$	40	17	43

into pairs and triplets leads to periodicity of 6 in the results, as shown in Table I.

V. GROUND-STATE ENERGY DISTRIBUTION

There are situations when only one state with given quantum numbers exists in the system. This includes the previously discussed example of d bosons (with seniority providing an additional quantum number), cases of an aligned state with $J_{\max}$, and many examples discussed in Appendix A where $D_{\ell,N} = 1$; we specifically mention there $J = 0$ triplets of bosons with even ℓ, which are unique ($D_{\ell,N=3} = 1$ for even ℓ), see Appendix A 2.

In these cases, the wave function $|\psi\rangle$ is uniquely determined by the state's quantum numbers, which makes the energy

$$E = \sum_L c_L V_L, \quad \text{where} \quad c_L = \sum_M \langle\psi|P^\dagger_{LM} P_{LM}|\psi\rangle, \tag{10}$$

a linear function of the interaction parameters V_L. Some discussion of analytically solvable models based on linearity is found in Ref. [20].

From the definition in Eq. (10), it is clear that

$$c_L \geqslant 0. \tag{11}$$

It is also clear that

$$\sum_L c_L = \frac{N(N-1)}{2} = \sigma_{\max}, \tag{12}$$

since, similar to the monopole interaction, Appendix B 1, this sum counts the total number of pairs in the state. We label this sum in Eq. (12) as $\sigma_{\max}$ because in the ensemble Eqs. (2),

$$\overline{E} = 0\,, \quad \overline{E^2} = \sum_L c_L^2, \tag{13}$$

and conditions Eqs. (12) and (11) constrain the width of the energy distribution

$$\frac{\sigma^2_{\max}}{\ell+1} \leqslant \overline{E^2} \leqslant \sigma^2_{\max}. \tag{14}$$

The minimum is realized when all $\ell + 1$ coefficients c_L are the same. The maximum, which is the most relevant limit for us, is realized for a pair condensate when only one c_L is nonzero. Thus, $\sigma^2_{\max}$ is the maximal energy variance that is possible for a state whose energy is a linear function of interaction parameters Eq. (10) in the two-body random ensemble Eqs. (2). Formation of a condensate that leads to a broad energy distribution reaching $\sigma_{\max}$ explains the preponderance of $J_{\max}$ being a ground state, as well as the enhanced chances of some other states with high spin.

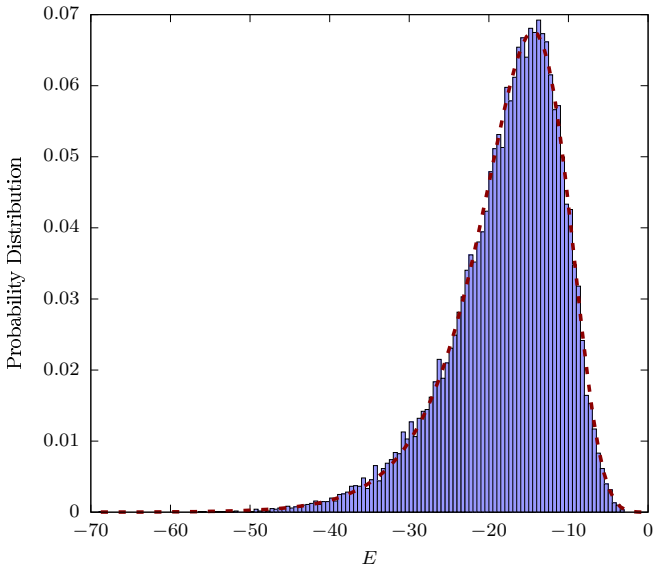

FIG. 4. Distribution of $J = 0$ ground-state energies in a system with $N = 8$ and $\ell = 8$. The distribution is compared with the Gumbel distribution in Eq. (15), where $a = -14.46(4)$ and $b = 0.183(2)$.

The energies of the ground states themselves are independent identically distributed variables; thus, their distribution follows one of three universal distributions [39–42]. Here we have a case of the Gumbel distribution

$$G(E) = b\,\exp[b(E-a) - \exp(b(E-a))] \tag{15}$$

because our random ensemble is given by interaction matrix elements with a normal distribution, and thus the probabilities of extreme values of energy fall faster than any power law. The numeric results are in very good agreement with Eq. (15). An example of the ground-state energy distribution is compared with the Gumbel function in Fig. 4. The parameters of the Gumbel distribution can be associated with the number of degrees of freedom [39,43,44].

For a Gaussian distribution, which is the case for Eq. (10) at the start of this discussion, the parameters of the distribution a and b depend on the size of the set of normally distributed random numbers from which the minimum or maximum is picked. We associate it with some effective dimensionality $\mathcal{D}$ of states competing to appear as ground states,

$$|a| = \sqrt{2\overline{E^2}}\,\mathrm{erf}^{-1}\left(\frac{\mathcal{D}-2}{\mathcal{D}}\right), \quad b = \mathcal{D} f(a), \tag{16}$$

where erf^{-1} denotes the inverse error function and function f is the normal distribution of energies E centered at zero and with variance $\overline{E^2}$. We discuss the minimum, thus a is negative.

Using the Gumbel distribution parameters a and b observed numerically and solving these equations allows us to determine the effective dimensionality $\mathcal{D}$ and the variance $\overline{E^2}$. In the limit of large $\mathcal{D}$, the expressions Eqs. (16) can be simplified using the product logarithm function, see Ref. [39]. In Table II, we include columns that, for each system, show the

TABLE II. Properties and numerical results for various systems. For numerical results, 100 000 realizations of the two-body random ensemble were used. Columns 1, 2, and 3 identify the system and the ground-state spin of interest, Sec. II. The next two columns show the number of states with spin J in a given system, $D_{\ell N}(J)$, and the total number of spin states, $D_{\ell N}$, see Appendix B. The following column shows $P(J)$ in percentage, see Sec. III. The following eight columns separated by double lines correspond to the discussion in Sec. VI. The parameters q_i listed in descending order can be interpreted as the probabilities of a previously determined fixed ith state to be a ground state; $D_{\rm gs}$ is the effective dimensionality of space spanned by the ground state. The last four columns separated by the second double line follow the discussion in Sec. V. They include two parameters of the Gumbel distribution in Eq. (15) and, extracted from these parameters, the number of states competing to be in the ground state $\mathcal{D}$ and the width of the energy distribution $\sqrt{\overline{E^2}}/\sigma_{\rm max}$ relative to the $\sigma_{\rm max} = N(N-1)/2$.

ℓ	N	J	$D_{\ell N}(J)$	$D_{\ell N}$	$P(J)$ [%]	q_1	q_2	q_3	q_4	q_4	q_6	q_7	$D_{\rm gs}$	a	b	$\mathcal{D}$	$\sqrt{\overline{E^2}}/\sigma_{\rm max}$
3	8	0	4	151	63.9	0.549	0.356	0.081					2.6	–8.49	0.162	5.7	0.33
4	8	0	7	526	39.8	0.562	0.161	0.087					2.6	–9.2	0.182	7	0.31
4	12	0	20	3788	64.2	0.391	0.339	0.172	0.049				4	–20.92	0.085	7.4	0.29
5	4	0	2	55	35.7	0.687	0.313						1.9	–3.64	0.599	9.6	0.48
5	5	5	10	141	41.3	0.497	0.194	0.177	0.053				4.2	–4.65	0.459	9.3	0.38
5	6	0	6	338	47.5	0.395	0.291	0.156	0.114				4.2	–6.6	0.321	9.2	0.36
5	7	5	34	734	40.9	0.482	0.177	0.166	0.078	0.051			4.7	–8.63	0.24	8.9	0.34
5	8	0	12	1514	33.9	0.6	0.218	0.127					3.1	–11.67	0.174	8.7	0.35
5	8	32	7	1514	1.1	0.513	0.486						2	–11.1	0.204	10.1	0.31
5	12	0	52	16660	42.6	0.45	0.173	0.146	0.1	0.053	0.03		5.4	–23.21	0.084	8.3	0.3
6	3	0	1	25	22.1	1							1	–2.566	0.859	9.7	0.67
6	4	0	3	86	49.1	0.457	0.381	0.162					2.8	–4.02	0.61	11.3	0.48
6	6	0	8	676	46.9	0.384	0.27	0.181	0.094				4.6	–8.26	0.287	10.8	0.41
6	7	6	63	1656	46.1	0.337	0.216	0.196	0.106	0.061	0.02		6.2	–10.36	0.228	12.4	0.21
6	8	0	20	3788	50.3	0.326	0.233	0.209	0.108	0.039	0.031		5.8	–13.6	0.173	10.7	0.37
6	9	0	28	8150	21.1	0.654	0.249	0.044					2.7	–17.02	0.136	10.4	0.36
6	12	0	127	61108	57.5	0.255	0.243	0.173	0.104	0.09	0.026	0.023	8	–28.4	0.079	10	0.34
7	4	0	3	126	38.5	0.463	0.364	0.173					2.8	–4.22	0.645	13.4	0.48
7	8	0	31	8512	39.3	0.34	0.176	0.126	0.106	0.096	0.072	0.021	7.3	–13.39	0.195	12.5	0.34
8	8	0	47	17575	24.1	0.446	0.153	0.127	0.086	0.074	0.028		6.3	–14.46	0.184	12.9	0.36
9	8	0	71	33885	36.7	0.254	0.154	0.113	0.087	0.067	0.056	0.038	13.5	–14.68	0.204	15.8	0.34

effective dimension $\mathcal{D}$ and the variance relative to its maximal value Eq. (14), namely, $\sqrt{\overline{E^2}}/\sigma_{\rm max}$. This is done by solving Eq. (16) given a and b from a numerical fit, such as the one shown in Fig. 4. Our studies show that due to the small dimensionality of $\mathcal{D}$, this procedure overestimates $\mathcal{D}$ and slightly underestimates $\sqrt{\overline{E^2}}$. For example, numerical studies of normal distributions that take as input unit width, $\sqrt{\overline{E^2}} = 1$, and $\mathcal{D} = 5, 6, 10, 100$ result in the corresponding list of $(\mathcal{D}, \sqrt{\overline{E^2}})$ being (6.5, 0.93), (7.5, 0.93) (12, 0.97) (106, 1); this gives an idea about the level of error in the inversion procedure. The two-body random ensemble is certainly more complicated, which is evident from the case of $N = 3$, $\ell = 6$ for $J = 0$, where it is analytically known from Eq. (A13) that $\sigma_{\rm max} = \sqrt{\overline{E^2}} = 3$, yet our procedure gives $\sqrt{\overline{E^2}} \approx 2$; as seen in Table II $\sqrt{\overline{E^2}}/\sigma_{\rm max} = 0.67$. Despite this, the results are certainly reflective of the width of the energy distribution and the number of states competing for the ground state position.

The following conclusions can be drawn from this discussion. First, in all cases studied, only about a dozen states are competing for the ground-state position, as evident from the values of $\mathcal{D}$ inferred from the distribution of ground-state energies. Compare $\mathcal{D}$ with $D_{\ell N}$ in Table II. Second, the width of the ground-state energy distribution is a substantial fraction of the maximum allowed value that occurs in condensates, indicating that only a few two-body matrix elements are responsible for the ground-state structure.

VI. GROUND-STATE WAVE FUNCTIONS

The previous analysis suggests that the states that appear as ground states are dominated by specific structures. For the following, let us consider W realizations from the random ensemble leading to a series of ground states $|\varphi_n\rangle$ with a particular spin J, where $n = 1, 2, \ldots, W$ labels each individual realization. As we are dealing with a particular angular momentum J, each of these wave functions can be expanded in $D = D_{\ell N}(J)$ basis states $|J_i\rangle$ which are eigenstates of J^2. To explain our procedure, let us suppose that most wave functions in the series $|\varphi_n\rangle$ are nearly the same, being close to some wave function $|\phi\rangle$ that can also be expanded as

$$|\phi\rangle = \sum_i c_i |J_i\rangle. \tag{17}$$

To find the best $|\phi\rangle$ from our ensemble, we should maximize the sum of all squared overlaps as a function of the unknown set $\{c_1, c_2, \ldots, c_D\}$,

$$\frac{1}{W}\sum_n |\langle\varphi_n|\phi\rangle|^2 = \sum_{i,k} c_i^* Q_{ik} c_k, \tag{18}$$

where the matrix element Q_{ik} is

$$Q_{ik} = \frac{1}{W}\sum_n \langle J_i|\varphi_n\rangle\langle\varphi_n|J_k\rangle. \tag{19}$$

The solution is well-known; the quadratic form in Eq. (18) is maximized for the largest eigenvalue of matrix Q. The eigenvector corresponding to the largest eigenvalue provides the solution for the set of coefficients $\{c_1, c_2, \ldots, c_D\}$.

Let q_i be a set of eigenvalues of Q organized in descending order for $i = 1, 2, \ldots, D$, and $|\phi_i\rangle$ be the corresponding eigenvector. As follows from Eq. (18), the matrix is positive definite so all eigenvalues q_i are positive. Moreover, as seen from Eq. (19), the trace is equal to one, so

$$\sum_i q_i = 1. \tag{20}$$

If all ground states $|\varphi_n\rangle$ actually had the same wave function, then the sum in Eq. (18) would be equal to one and the maximal eigenvalue of the factorized matrix Eq. (19) would be $q_1 = 1$ while the remaining eigenvalues would be equal to zero.

To highlight the meaning of these eigenvalues, let us imagine that each ground state $|\varphi_n\rangle$ from the random ensemble always exactly coincides with one of the wave functions $|\phi_i\rangle$. Then, the eigenvalue q_i represents a fraction describing how often a particular ith state happens to be a ground state.

In general, this interpretation provides an assessment of the dimensionality of space spanned by the ground states $|\varphi_n\rangle$. As seen in Table II, which includes the most prominent eigenvalues of matrix Q for each system, in most situations there are only a few large eigenvalues while all other ones are small. This indicates that, while the Hilbert space dimensionality given by $D_{\ell N}(J)$ can be very large, only a small fraction of these states appear as ground states. The effective dimensionality of the space spanned by the ground states can be evaluated using entropy

$$D_{\rm gs} = \exp(S), \quad \text{where} \quad S = -\sum_i q_i \ln(q_i). \tag{21}$$

The effective dimensionality $D_{\rm gs}$ is listed in Table II and is always much smaller than the total number of states of a given spin $D_{\ell N}(J)$.

Let us carry out the analysis of the ground-state wave functions to understand the minor preponderance of ground states with $J = (\ell - 1)N$. Consider the $\ell = 5$ and $N = 8$ system. As listed in Table II, the $J = 32$ ground state happens in about 1.1% of realizations, which is a lot given only seven states with this spin and 1514 possible spin states. Analysis of the eigenvalues of matrix Q shows that only two are effectively nonzero. It turns out that in this case the ground-state wave function is almost exclusively one of two possibilities, with corresponding probability for $|\phi_1\rangle$ being 51% and the probability for $|\phi_2\rangle$ being 49%. The realizations with $|\phi_2\rangle$ have $|\phi_2\rangle$ as a ground-state wave function exactly, with no admixtures. Some very small admixtures are present in realizations with $|\phi_1\rangle$. Assuming linearity and following Eqs. (10), (12), and (13) we find $\sqrt{\overline{E^2}}/\sigma_{\rm max} = 0.77$ and 0.71 for ϕ_1 and ϕ_2, respectively. The ϕ_1 relies on attractive matrix element V_{10}, while ϕ_2 emerges in the ground state due to attraction in V_8.

For the same $\ell = 5$ and $N = 8$ system, the $J = 0$ ground state happens in nearly 34% of random realizations. There are 12 $J = 0$ states in the system, and yet the effective dimensionality is only $D_{\rm gs} = 3$. This low dimensionality allows us to visualize the wave functions $|\varphi_n\rangle$ in Fig. 5 using a three-dimensional unit sphere. The nth wave function is shown by a point defined by the three components $\langle\phi_1|\varphi_n\rangle$, $\langle\phi_2|\varphi_n\rangle$, and $\langle\phi_3|\varphi_n\rangle$, which are the overlaps of $|\varphi_n\rangle$ with the principal eigenvectors of the Q matrix. The phase is selected so the first component is positive, thus all points are on the upper hemisphere. It is remarkable that the points are not covering the hemisphere uniformly; rather, they form a curve on the sphere, which indicates even further reduction of the measure of space spanned by the ground states. Considering $J = 0$ ground states of the Hamiltonians where only V_0 and V_2 are nonzero allows one to trace this curve, shown by the dashed line in Fig. 5. Special cases corresponding to quadrupole-quadrupole interaction (square), pairing (circle), and $V_2 = -1$ while everything else is zero (triangle) are shown. The highest density of points is in the vicinity of the quadrupole-quadrupole Hamiltonian ground state (square), while around pairing (circle) and $V_2 = -1$ (triangle) the density is low.

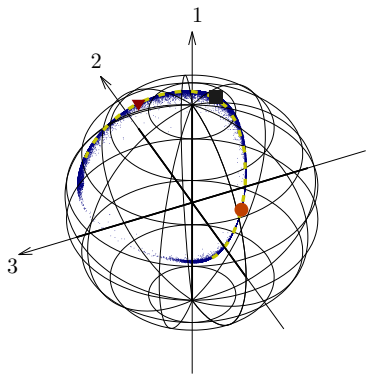

FIG. 5. Ground-state wave functions with $J = 0$ for a system of $N = 8$ $\ell = 5$ bosons are shown for the two-body random ensemble on a three-dimensional sphere. The dashed line traces the line formed by the $J = 0$ wave functions of the Hamiltonians containing only V_0 and V_2 matrix elements. Ground states corresponding to the quadrupole-quadrupole interaction Hamiltonian (square), Hamiltonian where $V_2 = -1$ while everything else is zero (triangle), and pairing (circle) are shown.

While some of these findings are specific to the systems considered, the analysis of ground-state wave functions shown in this section highlights that, out of the entire space of wave functions of a given J, those that appear as ground states span only a small subspace. Their structures are generally determined by a few matrix elements and their energy distribution variances, studied in the previous section, suggest condensate-type structures.

VII. CLUSTERING

As shown above, the ground states of randomly interacting systems of bosons are not uniformly random vectors in the Hilbert space; they are special, condensate-type structures and these properties allow them to have lower energy. The example of d bosons in Sec. IV, where all $J = 0$ states are either pair or triplet condensates, suggests that cluster condensates may be a general feature of boson systems. Oscillatory behavior as a function of the particle number seen in Fig. 3

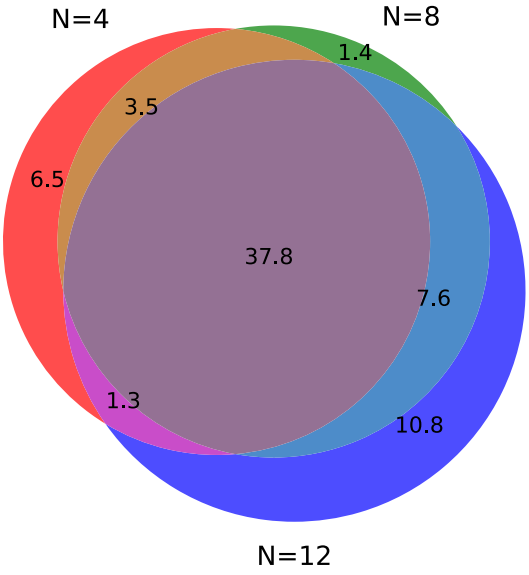

FIG. 6. Venn diagram showing the relationship between the sets of Hamiltonians from the two-body random ensemble that have a $J = 0$ ground state in the $N = 4$, $N = 8$, and $N = 12$ systems of $\ell = 6$ bosons. The numbers show percentage of the corresponding Hamiltonians from the total ensemble. The diagram is drawn to properly reflect the scale of sets and their overlaps.

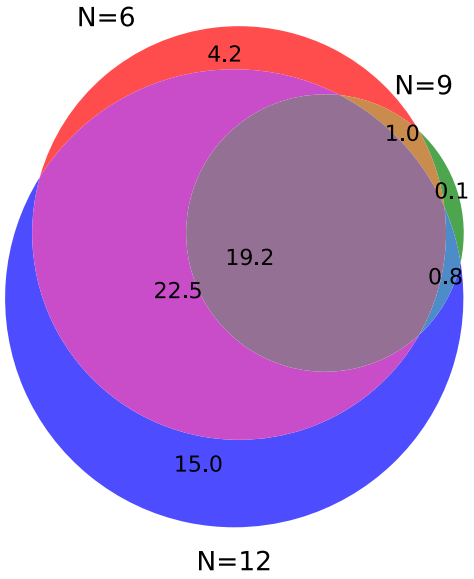

FIG. 7. Venn diagram, similar to Fig. 6, showing the set of Hamiltonians from the two-body random ensemble that have a $J = 0$ ground state in the $N = 6$, $N = 9$, and $N = 12$ systems of $\ell = 6$ bosons. The numbers show percentage of the corresponding Hamiltonians from the total ensemble. The diagram is drawn to properly reflect the scale of sets and their overlaps.

also supports the idea of triplets, quartets, or perhaps even bigger structures playing a role.

In what follows, we limit our study to $J = 0$ ground states in systems of $\ell = 6$ bosons. If, similar to d bosons, the $J = 0$ ground states are condensates, then systems with different numbers of clusters (but with the same Hamiltonian) should be similar; we explore this next.

Let us review the sets of Hamiltonians and their overlaps that produce the $J = 0$ ground states for various particle numbers. In Fig. 6, using a Venn diagram (also known as a set diagram), we show the set of Hamiltonians comprising the two-body random ensemble that amount to $J = 0$ ground states in $N = 4$, $N = 8$, and $N = 12$ systems of $\ell = 6$ bosons. The diagram reflects the sizes of the sets and their overlaps. All three systems are very similar. For example, the cases where, with the same interaction Hamiltonian, an $N = 4$ system has a $J = 0$ ground state but the ground-state spin of the $N = 8$ system is nonzero, are rare.

A slightly different situation is seen in Fig. 7 that compares the sets for $J = 0$ states in the $N = 6$, $N = 9$, and $N = 12$ systems of $\ell = 6$ bosons. All sets overlap covering $N = 9$. The $N = 3$ set is not shown in this figure, but its overlap with $N = 9$ is at the 90% level, indicating that in about 17% of overall cases we are dealing with spin zero triplets.

A. Pairing

It appears that pairs, triplets, and quartets are the most likely types of clusters. It is most instructive to start with pairs and pairing. Given that paired ground states are common in realistic situations, such as the superconducting ground state of fermions [45] or as a solution of the interacting boson model for nuclei [25], the prevalence of paired states is natural to expect. However, numerous studies with randomly interacting fermions show this not to be the case [19,46,47]. Our studies also show pairing not to be prevalent for randomly interacting bosons, with the exception of some very restrictive situations, such as with d bosons. As was already mentioned in the discussion related to Fig. 5, the number of realizations with paired ground states is low. This is evident from the low density of points around the paired state (orange circle) in Fig. 5.

In Fig. 8, we show the probability distribution for $\langle\varphi_n(N)|P^\dagger P|\varphi_n(N)\rangle$ (where we denote $P \equiv P_{00}$) for the $N = 12$ particle system. Since the eigenvalues of the pairing Hamiltonian are known analytically, Eq. (B5), and are associated via the seniority ν with the number of pairs, $\mathcal{N}_P = (N - \nu)/2$, we can assess the typical number of pairs. As evident from Fig. 8, there are many cases (about a quarter of realizations when the ground state is $J = 0$) with no pairs at all, while most of the remaining systems have about 3 pairs on average. This is far from the maximum of six pairs that corresponds to $\langle P^\dagger P\rangle = 138/13 \approx 10.6$.

B. Triplets

In a system with even ℓ, the three-boson state with spin $J = 0$ is unique, as mentioned in Appendix A 2. This allows us to uniquely define a triplet creation operator $T^\dagger \equiv T^\dagger_{00}$ that creates this state from the vacuum. Using the triplet creation and annihilation operators, we can assess the level of triplet clustering in the ground states and whether the ground states of different particle number are connected by triplet removal and addition.

In Fig. 9, we examine the removal of a triplet from the $J = 0$ ground state of the $N = 12$ particle system $T|\varphi_n(12)\rangle$.

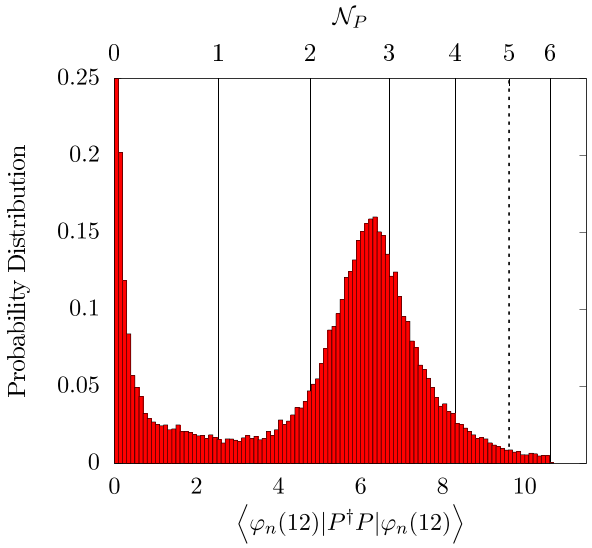

FIG. 8. The distribution of the pair number is shown for the $N = 12$ system of $\ell = 6$ bosons. The vertical lines show the values from Eq. (B5) for $\mathcal{N}_P = 0, 1, 2, \ldots, 6$ pairs. Technically, $\mathcal{N}_P = 5$ is not allowed for $J = 0$ states but its location is shown for reference.

For each nth realization of the ensemble, using a scatter plot, we show the overlap of the resulting state with the ground state of the $N = 9$ particle system squared $|\langle\varphi_n(9)|T|\varphi_n(12)\rangle|^2$ on the x axis and $\langle\varphi_n(12)|T^\dagger T|\varphi_n(12)\rangle$ on the y axis; the latter represents the norm of the state after triplet removal. All points in the figure appear very close to the diagonal line, meaning that the two quantities are nearly equal; thus, removal of a triplet from the $N = 12$ system leads to the ground state of the $N = 9$ system. Using a complete set of eigenstates in the $N = 9$ particle system labeled by i, the norm on the y axis

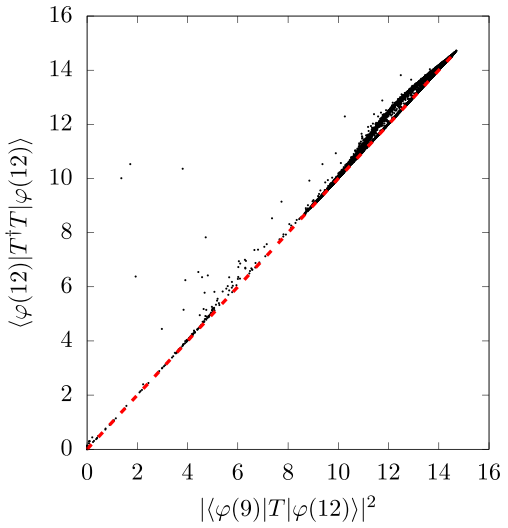

FIG. 9. Scatter plot that, for a 12-particle system of $\ell = 6$ bosons, shows triplet removal amplitude squared $|\langle\varphi(9)|T|\varphi(12)\rangle|^2$ versus normalization $\langle\varphi(12)|T^\dagger T|\varphi(12)\rangle$. When triplet removal identically leads to the ground state of the $N = 9$ system $|\varphi(9)\rangle = T|\varphi(12)\rangle$, the two quantities are equal; this condition is shown by a dashed diagonal line.

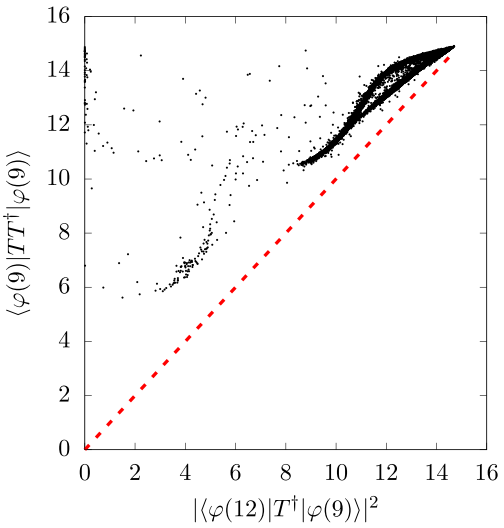

FIG. 10. This figure is similar to Fig. 9 but considers triplet addition to the $N = 9$ system; $|\langle\varphi(12)|T^\dagger|\varphi(9)\rangle|^2$ versus normalization $\langle\varphi(9)|TT^\dagger|\varphi(9)\rangle$. When triplet addition leads to the ground state of the $N = 12$ system $|\varphi(12)\rangle = T^\dagger|\varphi(9)\rangle$, the two quantities are equal and the scattered points appear on a diagonal line.

can be expanded as

$$\langle\varphi_n(12)|T^\dagger T|\varphi_n(12)\rangle = \sum_i |\langle\varphi_n^{(i)}(9)|T|\varphi_n(12)\rangle|^2. \quad (22)$$

The result shows that a single term with the index i corresponding to the ground state dominates this sum.

In Fig. 10, we show the addition of a triplet to the nine-particle system, $T^\dagger|\varphi_n(9)\rangle$. The results are similar, although some deviations indicate that the ground states of 12-particle systems have some small additional components that make $|\varphi_n(12)\rangle$ slightly different from $T^\dagger|\varphi_n(9)\rangle$. More deviations in the case of cluster addition as compared to cluster removal appear to be a general feature that we observed for other systems as well. They could be caused by the presence of different cluster types—we discuss quartets in what follows—or by other phenomena.

To study the number of triplets in the ground states, in Fig. 11 we show the distribution of $\langle\varphi_n(12)|T^\dagger T|\varphi_n(12)\rangle$, which appeared on the y axis in Fig. 9 for the $N = 12$ system. Similar to pairing studied in Fig. 8, this quantity is to be interpreted as the cluster number. However, unlike for pairing, there are no analytic eigenvalues for the triplet number operator $T^\dagger T$. Therefore, we diagonalize $T^\dagger T$ numerically. Similar to Fig. 8, the eigenvalues of $T^\dagger T$ are shown by vertical lines in Fig. 11. We expect the $J = 0$ states in the 12-particle system to have zero, one, two, or four triplets. Note that a spin-zero state with three triplets is not possible because three remaining particles must also have spin zero and thus form a fourth triplet. Out of 127 $J = 0$ states in the system, there are 100 zero eigenvalues that we associate with no triplets at all, $\mathcal{N}_T = 0$. The unique largest eigenvalue of about 15 clearly corresponds to the full condensate of $\mathcal{N}_T = 4$ triplets. The remaining eigenvalues correspond to intermediate situations but, given clear visible gaps, we can roughly assign those between about 7 and 10 as corresponding to two triplets and

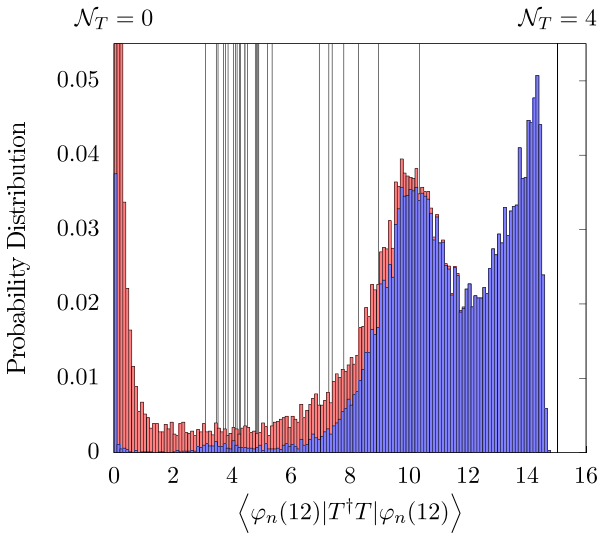

FIG. 11. The distribution of the triplet number is shown for the $N = 12$ system of $\ell = 6$ bosons. The vertical lines show eigenvalues of the triplet number operator. The histogram in red shows all 58% of realizations with a $J = 0$ ground state; the histogram in blue corresponds to those 19% of ensemble realizations where $N = 6$ and 9 particle systems also have a $J = 0$ ground state.

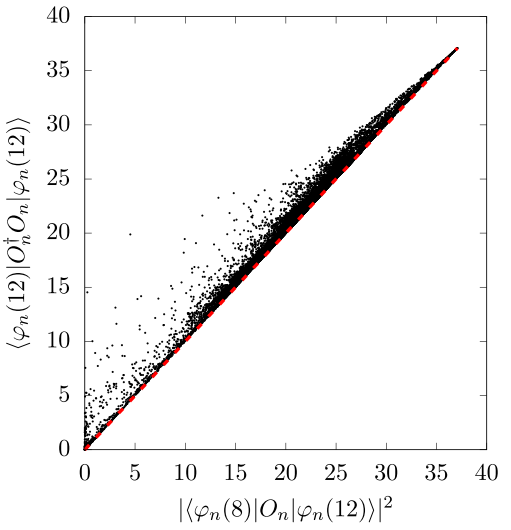

FIG. 12. This figure is similar to Fig. 9 but considers a quartet removal from an $N = 12$ system. Unlike with the triplets, the quartet is defined for each random realization using a ground state of a four-particle system. Only those cases are studied where all systems involved, the $N = 4$, 8, and 12 systems, have a $J = 0$ ground state. This happens in 37.8% of realizations, as seen in the Venn diagram Fig. 6.

those between about 3 and 5 to one triplet. The red histogram shows all cases (about 60% of realizations) when $J = 0$ is the ground state in the 12-particle system. Out of these, the blue histogram shows the cases when the same realization also gives a $J = 0$ ground state in the $N = 6$ and $N = 9$ systems, which is about 20% of realizations, see Venn diagram Fig. 6. The peak near the maximum triplet number indicates that many of these systems (about 10% of all realizations) are nearly a perfect triplet condensate state. Note that this result is very different from that seen in Fig. 8 for pairing.

The other peak in the probability distribution near zero for red cases shows that, where most realizations of six- or nine-particle systems or both do not have a spin $J = 0$ ground state, the $J = 0$ ground state of the 12-particle system has no triplets. The fraction of these realizations that possess $J = 0$ ground states along with $N = 4$ and $N = 8$ systems, see Fig. 6, is about 38% and the peak in Fig. 11 near zero ($\langle\varphi_n(12)|T^\dagger T|\varphi_n(12)\rangle < 0.8$) comprises 35% of realizations. As we discuss in the following subsection, the structure of those systems is dominated by quartets.

C. Quartets

Quartets are more difficult to address since, generally, an $N = 4$ system has several states with spin $J = 0$, for example, $D_{\ell=6,N=4}(0) = 3$. One of these states is associated with pairing while the other two offer different types of possible quartets. Whichever structure dominates in the ground state is determined by the Hamiltonian. As seen from the data in Table II, the effective dimensionality $D_{\rm gs} = 2.8$, so all three $J = 0$ states appear as ground states relatively often. Thus, for the study of quartets, we define the quartet operator individually for each realization using the corresponding $J = 0$ ground state of the four-particle system, so

$$O_n^\dagger|0\rangle \equiv |\varphi_n(4)\rangle. \tag{23}$$

Our results in Figs. 12 and 13, similar to the previously considered triplets in Figs. 9 and 10, show that the ground states of these systems are close to those formed by a repeated action of the quartet operator:

$$|\varphi_n(8)\rangle \propto O_n^\dagger|\varphi_n(4)\rangle = (O_n^\dagger)^2|0\rangle, \tag{24}$$

$$|\varphi_n(12)\rangle \propto O_n^\dagger|\varphi_n(8)\rangle \propto (O_n^\dagger)^3|0\rangle. \tag{25}$$

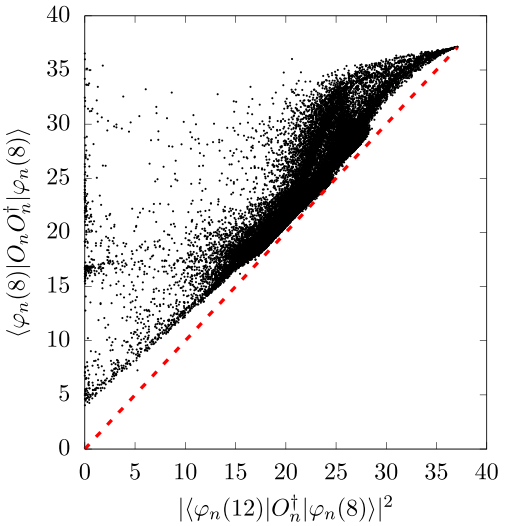

FIG. 13. This figure is similar to Fig. 12, but for quartet addition to the ground state of the $N = 8$ system.

Thus, the ground states in larger systems are created from an $N = 4$ ground state by replicating the quartet several times, which of course is not a problem for bosons.

Finally, commenting on the structure of the $N = 12$ systems, we can summarize that the $J = 0$ ground state happens in about 58% of cases, and out of those 16% are dominated by triplet structure (with 10% being in nearly perfect four-triplet condensate state) and about 38% by quartets. The overlap between the two types of structures is small.

VIII. CONCLUSIONS

Random two-body ensembles provide a unique perspective on the general emergence of phenomena in quantum many-body physics where out of randomness and complexity unique features, new degrees of freedom, and collective dynamics emerge. The main finding of this paper is that the ground states of bosonic two-body random ensembles are not actually random.

First, what has been known for some time: the statistics of spins of states that appear as ground states are dominated by spin zero for even-particle systems and by a single-boson spin for odd-particle systems [20,29–32]. The chances of seeing the most aligned state with the maximum spin possible are also enhanced, but the coherent boson-condensate structure of that is known.

Second, our numerical study of the ground-state energy distribution using extreme value distribution theory shows that out of all states in the spectrum, only about a dozen actually compete to be in the ground state. Moreover, all of these states are collective and their energies scale with the number of pairs $\propto N^2$.

Third, the analysis of the ground-state wave functions shows that they span a very small subspace out of the total allowed Hilbert space. As seen in Table II, roughly 80% of ground-state wave functions are comprised of linear combinations of two components.

Finally, we find that the above results for $J = 0$ are largely explained by the formation of condensates of clusters, mainly dominated by spin-zero triplets and quartets. For spin-zero triplets, which are uniquely defined, numerical studies show that ground states of adjacent systems N and $N \pm 3$ are connected by triplet removal and triplet addition; and study of the distribution of the triplet number operator support that a large fraction of ground states are triplet condensates. Similar results are seen for quartets; in that case, the $J = 0$ ground states of large systems with $N = 8$ and 12 have a structure built from the $N = 4$ system by repeating it two and three times, respectively.

There are certainly questions that remain outside the scope of this paper, including how these results extrapolate for larger systems and whether larger clusters play a significant role. It is also interesting that while the interaction is two-body, pairing does not play a more significant role; reorganization of particles into clusters of more than two particles clearly appears to be more favorable. The main conclusion of our study is that the emergence of correlated structures in quantum many-body systems of identical particles is highly probable even though their interactions are random.

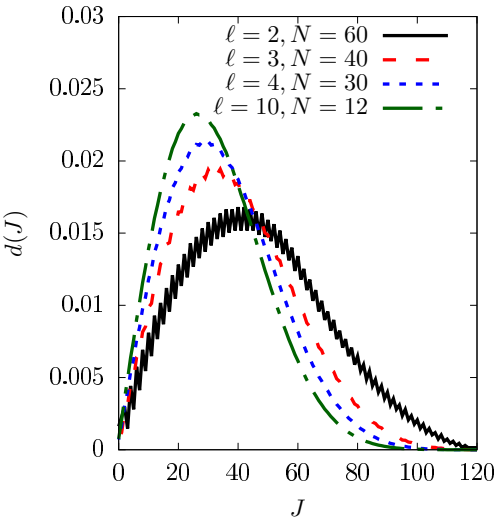

FIG. 14. The fraction of states of a given spin J is shown for several different systems.

ACKNOWLEDGMENT

This material is based upon work supported by the U.S. Department of Energy Office of Science, Office of Nuclear Physics under Award No. DE-SC0009883.

APPENDIX A: BOSONIC GEOMETRY

The question of spin statistics, namely, how many states of a given spin there are in a many-body system addresses the geometry of the Hilbert space, which is independent from the interaction Hamiltonian. We define $D_{\ell N}(J)$ to be the number of states with spin J (multiplets of $2J + 1$ projections) in the system of N identical bosons of spin ℓ. Then, the dimensionality of the Hilbert space is

$$D' = \sum_J (2J+1) D_{\ell N}(J) = \frac{(2\ell+N)!}{(2\ell)!N!}, \tag{A1}$$

where the prime indicates a quantity that accounts for magnetic substates. For convenience of comparison, we define the total number of states in the system (not including magnetic degeneracies) as

$$D_{\ell N} = \sum_J D_{\ell N}(J), \tag{A2}$$

and the fraction of states of a given J as

$$d(J) = \frac{D_{\ell N}(J)}{D_{\ell N}}. \tag{A3}$$

In Fig. 14, we show $d(J)$ as a function of J for several systems. This is a peaked distribution showing that the fraction of states with low spins and high spins is low.

The distribution of magnetic projections M, which is the sum of magnetic projections of individual particles, due to the central limit theorem, is expected to be nearly Gaussian, see Refs. [33,48]. Then, having

$$D'(M) = D' \sqrt{\frac{\beta}{\pi}} e^{-\beta M^2}, \tag{A4}$$

the number of states with a given J is

$$D_{\ell N}(J) = D'(M = J) - D'(M = J + 1), \tag{A5}$$

which results in

$$D_{\ell N}(J) \approx D'\beta\sqrt{\frac{\beta}{\pi}}(2J+1)\, e^{-\beta J(J+1)} \tag{A6}$$

and

$$d(J) \approx \beta(2J+1)\, e^{-\beta J(J+1)}. \tag{A7}$$

This describes well the results shown in Fig. 14.

The bosonic nature of particles allows only for fully symmetric states. This restriction amounts to slight modification of the distribution Eq. (A4), making it sub-Gaussian (platykurtic) with reduced tails.

1. Special structures

The fully aligned state with the maximum spin $J_{\max}$ is unique:

$$D_{\ell N}(J_{\max}) = 1, \quad \text{where} \quad J_{\max} = N\ell. \tag{A8}$$

For any unique state when $D_{\ell N}(J) = 1$, the energy is a linear function of the interaction parameters V_L. For an aligned state, a condensate of bosons all with the same maximum or minimum magnetic projections, the energy from two-body interactions is

$$E = \frac{N(N-1)}{2} V_{2\ell}. \tag{A9}$$

The factor $N(N-1)/2$ reflects the number of pairs in the condensate of aligned bosons.

There is no state with $J = \ell N - 1$ and there are always unique states with $J = \ell N - 2$ and with $J = \ell N - 3$.

A remarkable symmetry exists between systems of even number N bosons with spin ℓ and 2ℓ bosons each with spin $N/2$, namely, between (ℓ, N) and $(\ell' = N/2, N' = 2\ell)$. As follows from Eq. (A1), these systems have an identical number of states and an identical maximum $J_{\max} = \ell N = \ell' N'$. These two Hilbert spaces break down into an identical number of irreducible representations of the rotational group. Thus,

$$D_{\ell,\,N}(J) = D_{N/2,\,2\ell}(J), \quad \text{where } N \text{ is even.} \tag{A10}$$

In general, the number of states with a certain angular momentum is not known analytically, but there are special cases. For $N = 2$, the result is trivially $D_{\ell N=2}(J) = 1$ and $D_{\ell N=2} = \ell + 1$.

2. System of three bosons

For three bosons, the sequence $D_{\ell,N=3}(J)$ as a function of J is actually universal up to $J = \ell + 1$, which is to say that $D_{\ell,N=3}(J)$ does not depend on ℓ as long as $J \leqslant \ell + 1$. We found a simple relation,

$$D_{\ell,N=3}(J) = D_{\ell-2,N=3}(J) + \begin{cases} 1 & \text{for } \ell \leqslant J \leqslant 3\ell \text{ and } J \neq 3\ell - 1 \\ 0 & \text{otherwise,} \end{cases} \tag{A11}$$

that allows one to establish the number of states of each spin analytically. The above relation also implies that the sequence is unique near the terminating highest angular momentum $J = 3\ell$; in particular, $D_{\ell,N=3} = 1, 0, 1, 1, 1, 1, 2...$ for $J = 3\ell,\ 3\ell - 1,\ 3\ell - 2, \ldots$. Using this recurrence relation, we can find the total number of J states $D_{\ell,N}$ for even and odd ℓ bosons. This is given by

$$D_{\ell,N=3} = \frac{1}{2}(\ell+1)^2 + \begin{cases} \frac{1}{2} & \text{for even } \ell \\ 0 & \text{for odd } \ell. \end{cases} \tag{A12}$$

For $N = 3$ odd-parity bosons, the recurrence Eq. (A11) starts with $\ell = 1$ implying that three bosons of any odd angular momentum ℓ cannot couple to $J = 0$ and to $J = 2$, which is similar to Furry's theorem.

For three bosons of even parity (starting with $\ell = 2$), $J = 1$ is not possible and states with $J = 0, 2, 3$, and 5 (assuming $\ell > 2$) are unique. The energy of the unique $J = 0$ state is

$$E_0 = 3V_\ell. \tag{A13}$$

3. Spin $\ell = 1$ bosons

For a system of bosons with $\ell = 1$, the $D_{\ell=1N}(J) = 1$ for $J = N,\ N-2, \ldots,\ 0$ or 1 and zero otherwise. This property is well-known for the case of the three-dimensional harmonic oscillator where, for each shell, $N = 2n + J$, where the number of quanta N is represented by the number of bosons and n is an integer. It is also possible to think about the structure of aligned states with magnetic projection $M = J$ as being a two-condensate system: n boson pairs coupled to $L = 0$ are combined with an aligned state of $N - 2n$ spin $\ell = 1$ bosons, giving a total angular momentum of $J = N - 2n$.

4. Spin $\ell = 2$ bosons

The number of different spin states for d bosons can be worked out by considering it as a mixture of two spinless condensates with free particles: $\mathcal{N}_P$ of $J = 0$ pairs and $\mathcal{N}_T$ of $J = 0$ triplets, so $N = 2\mathcal{N}_P + 3\mathcal{N}_T + f$, where f represents the number of remaining particles not included into the spinless condensates. These uncoupled f particles are the ones producing the angular momentum

$$J = 2f,\ 2f-2,\ 2f-3,\ 2f-4, \ldots,\ f, \tag{A14}$$

which can take all integer values between $2f$ and f with the exception of $2f - 1$.

It is clear that similar condensates of spinless clusters appear as a generic feature of bosonic many-body states, but the number of different kinds of spinless clusters grows very fast and, at some moment, the condensates are no longer orthogonal. For $\ell = 2$, the number of $J = 0$ states can be found as the number of ways the total number of particles can be broken into pairs and triplets, i.e., the number of all possible pairs $\{\mathcal{N}_P, \mathcal{N}_T\}$ so $2\mathcal{N}_P + 3\mathcal{N}_T = N$.

5. Spin $\ell = 3$ bosons

For $\ell = 3$, there is no known analytical result, but organization into clusters is still useful. Considering $D_{\ell=3N}(0)$ as a

function of the particle number N, we find that, up to $N = 30$ particles, all states with $J = 0$ can be represented by spinless clusters with sizes of 2, 4, 6, 10, and 15 bosons—only for $N = 30$ $D_{\ell=3,N=30}(0) = 47$, whereas there are 48 different sets of $\{\mathcal{N}_2, \mathcal{N}_4, \mathcal{N}_6, \mathcal{N}_{10}, \mathcal{N}_{15}\}$ possible. Here we use $\mathcal{N}_n$ to denote a number of spinless clusters of n bosons ($\mathcal{N}_2 = \mathcal{N}_P$ in our other notation). Most likely, this implies that a pair of two spinless 15-boson clusters can be represented as condensates of other types.

For $\ell = 3$, the largest system with no $J = 0$ states is for $N = 13$, $D_{\ell=3\,N=13}(0) = 0$.

6. Other special cases

For $N = 4$, the states with $J = 4\ell$, $4\ell - 2$, $4\ell - 3$, and $4\ell - 5$ are unique. Other nontrivial cases worth mentioning are $(\ell, N) = (5, 5)$, $(5, 7)$ and (7,5), all have no $J = 0$ states. Apart from the already mentioned triplet $(\ell, N) = (2, 3)$, a single $J = 0$ state appears in (3,15), (3,17), (9,5), and (11,5). As mentioned earlier, energies of these states are linear functions of interaction parameters. For example, the state of 15 bosons with spin 3 has energy

$$E = \tfrac{240}{7}V_2 + \tfrac{2925}{77}V_4 + \tfrac{360}{11}V_6. \tag{A15}$$

APPENDIX B: SPECIAL HAMILTONIANS

There are several important special cases of the two-body interaction Hamiltonian Eq. (1) that allow for analytic solutions.

1. Monopole interaction

If all matrix elements of the two-body interaction are the same,

$$V_L^{(m)} = 1, \tag{B1}$$

we have the monopole Hamiltonian $H^{(m)}$. In this case, the pairwise interactions are not sensitive to the types of pairs. Energies of all many-body states are equal and given by the number of pairs that can be formed from N particles:

$$E^{(m)} = \tfrac{1}{2}N(N-1). \tag{B2}$$

2. Pairing

Pairs of angular momentum $L = 0$, whose operators we denote without subscripts $P \equiv P_{00}$, are special from the symmetry perspective and can serve as building blocks for a collective $J = 0$ pair condensate state. For a single type of bosons, the commutator of pair operators is

$$[P, P^\dagger] = \frac{2\ell + 1 + 2N}{2\ell + 1}. \tag{B3}$$

Because of this algebraic property, the pairing Hamiltonian $H^{(p)} = P_{00}^\dagger P_{00}$, defined with a set of matrix elements

$$V_L^{(p)} = \delta_{L0}, \tag{B4}$$

has eigenvalues

$$E^{(p)} = \frac{(N-\nu)(N+\nu+2\ell-1)}{2(2\ell+1)}, \tag{B5}$$

where ν is the seniority given by the number of unpaired particles. The $N - \nu$ particles create a single paired state of zero angular momentum while the ν unpaired particles do not participate in the interactions at all but add degeneracy and angular momentum to the state.

3. Rotational Hamiltonian

The square of the angular momentum operator $\mathbf{J}^2$ can also be constructed using the general form in Eq. (1) plus a one-body term proportional to the number of particles:

$$\mathbf{J}^2 = \ell(\ell+1)N + H^{(j)}. \tag{B6}$$

Here, the two-body part $H^{(j)}$ is defined by matrix elements:

$$V_L^{(j)} = L(L+1) - 2\ell(\ell+1). \tag{B7}$$

The eigenvalues of $H^{(j)}$ are

$$E^{(j)} = J(J+1) - \ell(\ell+1)N. \tag{B8}$$

APPENDIX C: PRIMED ENSEMBLE

Any Hamiltonian Eq. (1) always commutes with $H^{(j)}$ and $H^{(m)}$ because angular momentum and particle number are conserved quantities. For this reason, the removal of these two components does not change any structure of the wave functions, namely, for any α and γ, the Hamiltonian given by

$$H' = H - \alpha H^{(m)} - \gamma H^{(j)} \tag{C1}$$

has wave functions identical to those of H; the relationship between energies is

$$E'_J = E_J - \frac{\alpha}{2}N(N-1) - \gamma[J(J+1) - \ell(\ell+1)N]. \tag{C2}$$

The transformation in Eq. (C1) in terms of matrix elements of Eq. (1) is

$$V'_L = V_L - \alpha - \gamma[L(L+1) - 2\ell(\ell+1)]. \tag{C3}$$

The $\gamma = 0$ case amounts to an identical ensemble where in each realization all energies are shifted by a constant.

We determine α and γ from a set of V_L by minimizing the sum $\sum_L (2L+1)V_L'^2$, which amounts to a fitting of all two-particle states, including their magnetic substates. We define the monopole term

$$M = \frac{\sum(2L+1)V_L}{\sum(2L+1)} \tag{C4}$$

and angular momentum term

$$F = \frac{\sum(2L+1)[L(L+1) - 2\ell(\ell+1)]V_L}{\sum(2L+1)[L(L+1) - 2\ell(\ell+1)]}. \tag{C5}$$

The minimization procedure determines α and γ as

$$\gamma = \frac{3(F-M)}{(2\ell+3)(\ell+2)(2\ell-1)} \tag{C6}$$

and

$$\alpha = M - \gamma\ell. \tag{C7}$$

[1] E. P. Wigner, Characteristic vectors of bordered matrices with infinite dimensions, Ann. Math. **62**, 548 (1955).

[2] E. P. Wigner, Characteristic vectors of bordered matrices with infinite dimensions II, Ann. Math. **65**, 203 (1957).

[3] E. P. Wigner, On the distribution of the roots of certain symmetric matrices, Ann. Math. **67**, 325 (1958).

[4] T. Guhr, A. Muller-Groeling, and H. A. Weidenmuller, Random-matrix theories in quantum physics: Common concepts, Phys. Rep. **299**, 189 (1998).

[5] H. A. Weidenmüller and G. E. Mitchell, Random matrices and chaos in nuclear physics: Nuclear structure, Rev. Mod. Phys. **81**, 539 (2009).

[6] G. Akemann, J. Baik, and P. D. Francesco, *The Oxford Handbook of Random Matrix Theory*, online ed., Oxford Handbooks in Mathematics (Oxford University Press, New York, 2015).

[7] V. K. B. Kota, Embedded random matrix ensembles for complexity and chaos in finite interacting particle systems, Phys. Rep. **347**, 223 (2001).

[8] O. Bohigas and J. Flores, Two-body random hamiltonian and level density, Phys. Lett. B **34**, 261 (1971).

[9] T. A. Brody, J. Flores, J. B. French, P. A. Mello, A. Pandey, and S. S. M. Wong, Random-matrix physics: Spectrum and strength fluctuations, Rev. Mod. Phys. **53**, 385 (1981).

[10] J. B. French and S. S. M. Wong, Validity of random matrix theories for many-particle systems, Phys. Lett. B **33**, 449 (1970).

[11] J. B. French and S. S. M. Wong, Some random-matrix level and spacing distributions for fixed-particle-rank interactions, Phys. Lett. B **35**, 5 (1971).

[12] V. G. Zelevinsky, Mean-field out of chaos, Nucl. Phys. A **555**, 109 (1993).

[13] V. V. Flambaum, A. A. Gribakina, G. F. Gribakin, and M. G. Kozlov, Structure of compound states in the chaotic spectrum of the ce atom: Localization properties, matrix elements, and enhancement of weak perturbations, Phys. Rev. A **50**, 267 (1994).

[14] V. Zelevinsky, B. A. Brown, N. Frazier, and M. Horoi, The nuclear shell model as a testing ground for many-body quantum chaos, Phys. Rep. **276**, 85 (1996).

[15] C. W. Johnson, G. F. Bertsch, and D. J. Dean, Orderly Spectra from Random Interactions, Phys. Rev. Lett. **80**, 2749 (1998).

[16] V. Zelevinsky and A. Volya, Chaotic features of nuclear structure and dynamics: Selected topics, Phys. Scr. **91**, 033006 (2016).

[17] V. Abramkina and A. Volya, Quadrupole collectivity in the two-body random ensemble, Phys. Rev. C **84**, 024322 (2011).

[18] V. Zelevinsky and A. Volya, Nuclear structure, random interactions and mesoscopic physics, Phys. Rep. **391**, 311 (2004).

[19] D. Mulhall, A. Volya, and V. Zelevinsky, Geometric Chaoticity Leads to Ordered Spectra for Randomly Interacting Fermions, Phys. Rev. Lett. **85**, 4016 (2000).

[20] P. Chau Huu-Tai, A. Frank, N. A. Smirnova, and P. Van Isacker, Geometry of random interactions, Phys. Rev. C **66**, 061302(R) (2002).

[21] Y. M. Zhao, A. Arima, and N. Yoshinaga, Simple approach to the angular momentum distribution in the ground states of many-body systems, Phys. Rev. C **66**, 034302 (2002).

[22] T. Papenbrock and H. A. Weidenmuller, Distribution of Spectral Widths and Preponderance of Spin-0 Ground States in Nuclei, Phys. Rev. Lett. **93**, 132503 (2004).

[23] Y. M. Zhao, A. Arima, and N. Yoshinaga, Regularities of many-body systems interacting by a two-body random ensemble, Phys. Rep. **400**, 1 (2004).

[24] C. W. Johnson and H. A. Nam, New puzzle for many-body systems with random two-body interactions, Phys. Rev. C **75**, 047305 (2007).

[25] A. Arima and F. Iachello, The interacting boson model, Annu. Rev. Nucl. Part. Sci. **31**, 75 (1981).

[26] R. Bijker and A. Frank, Band Structure from Random Interactions, Phys. Rev. Lett. **84**, 420 (2000).

[27] R. Bijker and A. Frank, Regular spectra in the vibron model with random interactions, Phys. Rev. C **65**, 044316 (2002).

[28] P. Cejnar and J. Jolie, Quantum phase transitions in the interacting boson model, Prog. Part. Nucl. Phys. **62**, 210 (2009).

[29] Y. M. Zhao, A. Arima, and N. Yoshinaga, Angular momentum distribution of the ground states in the presence of random interactions: Boson systems, Phys. Rev. C **68**, 014322 (2003).

[30] Y. Lu, Y. M. Zhao, and A. Arima, Spin I ground state probabilities of integrable systems under random interactions, Phys. Rev. C **91**, 027301 (2015).

[31] G. J. Fu, Y. Zhang, Y. M. Zhao, and A. Arima, Collective modes of low-lying states in the interacting boson model with random interactions, Phys. Rev. C **98**, 034301 (2018).

[32] Y. M. Zhao, Regularity of atomic nuclei with random interactions: Sd bosons, Front. Phys. **13**, 132114 (2018).

[33] V. Zelevinsky and A. Volya, *Physics of Atomic Nuclei* (Wiley-VCH, Weinheim, 2017).

[34] C. White, Ph.D. thesis, Florida State University, 2023.

[35] D. S. Dean and S. N. Majumdar, Large Deviations of Extreme Eigenvalues of Random Matrices, Phys. Rev. Lett. **97**, 160201 (2006).

[36] F. Iachello and A. Arima, *The Interacting Boson Model* (Cambridge University Press, Cambridge, 1987).

[37] R. F. Casten, *Algebraic Approaches to Nuclear Structure: Interacting Boson and Fermion Models*, 1st ed., Contemporary Concepts in Physics (Harwood Academic Publishers, 1993; CRC Press, Boca Raton, 2019).

[38] A. Frank, P. V. Isacker, and J. Jolie, *Symmetries in Atomic Nuclei: From Isospin to Supersymmetry*, 1st ed. (Springer-Verlag, New York, 2009).

[39] A. Hansen, The three extreme value distributions: An introductory review, Front. Phys. **8**, 604053 (2020).

[40] J. Beirlant, Y. Goegebeur, J. Segers, J. Teugels, D. D. Waal, and C. Ferro, *Statistics of Extremes: Theory and Applications*, 1st ed. (Wiley, Chichester, 2004).

[41] J. Galambos, *The Asymptotic Theory of Extreme Order Statistics*, 2nd ed. (Robert E. Krieger Publishing Company, Malabar, 1987).

[42] E. J. Gumbel, *Statistics of Extremes* (Columbia University Press, New York, 1958).

[43] V. K. B. Kota and N. D. Chavda, Embedded random matrix ensembles from nuclear structure and their recent applications, Int. J. Mod. Phys. E. **27**, 1830001 (2018).

[44] M. Palassini, Ground-state energy fluctuations in the Sherrington-Kirkpatrick model, J. Stat. Mech. Theory Exp. (2008) P10005.

[45] R. A. Broglia and V. Zelevinsky, *Fifty Years of Nuclear BCS*, edited by R. A. Broglia and V. Zelevinsky (World Scientific, Singapore, 2013), p. 670.

[46] V. Zelevinsky and A. Volya, Random interactions and ground state spin of finite fermi systems, Int. J. Mod. Phys. B **20**, 2730 (2006).

[47] V. G. Zelevinsky, D. Mulhall, and A. Volya, Do we understand the role of incoherent interactions in many-body physics? Phys. At. Nucl. **64**, 525 (2001).

[48] T. Ericson, The statistical model and nuclear level densities, Adv. Phys. **9**, 425 (1960).